| Journal of Coastal Research | 11 | 4 | 1062–1074 | Fort Lauderdale, Florida | Fall 1995 |
|---|---|---|---|---|---|

# Stability Shear Stress and Equilibrium Cross-Sectional Geometry of Sheltered Tidal Channels

**Carl T. Friedrichs**

College of William and Mary
School of Marine Science
Virginia Institute of Marine Science
Gloucester Point, VA 23062, U.S.A.

## ABSTRACT

FRIEDRICHS, C.T., 1995. Stability shear stress and equilibrium cross-sectional geometry of sheltered tidal channels. *Journal of Coastal Research*, 11(4), 1062–1074. Fort Lauderdale (Florida), ISSN 0749-0208.

This study relates tidal channel cross-sectional area (A) to peak spring discharge (Q) via a physical mechanism, namely the stability shear stress ($\tau_S$) just necessary to maintain a zero gradient in net along-channel sediment transport. It is assumed that if bed shear stress ($\tau$) is greater than $\tau_S$, net erosion will occur, increasing A, and reducing $\tau \sim (Q/A)^2$ back toward $\tau_S$. If $\tau < \tau_S$ there will be net deposition, reducing A and increasing $\tau$ toward $\tau_S$. A survey of the literature allows estimates of Q and A at 242 sections in 26 separate sheltered tidal systems. Assuming a single value of $\tau_S$ characterizes the entire length of a given tidal channel, it is predicted that along-channel geometry will follow the relation $Ah_R^{1/6} \sim Q$. Along-channel regressions of the form $Ah_R^{1/6} \sim Q^{\beta}$ give a mean observed value for $\beta$ of 1.00 ± 0.06, which is consistent with this concept. Results indicate that a lower bound on $\tau_S$ (and an upper bound on A) for stable channels is provided by the critical shear stress ($\tau_C$) just capable of initiating sediment motion. Observed $\tau_S$ is found to vary among all systems as a function of spring tidal range ($R_{sp}$) according to the relation $\tau_S \approx 2.3\, R_{sp}^{0.79}\, \tau_C$. Observed deviations from uniform $\tau_S$ along individual channels are associated with along-channel variation in the direction of maximum discharge (i.e., flood- versus ebb-dominance).

ADDITIONAL INDEX WORDS: *Estuaries, tides, morphodynamics.*

## INTRODUCTION

Feedback between tidal channel morphology and tidal flow properties has long been recognized by coastal engineers and geologists (see text by BRUUN, 1978, for example). Deepening of tidal channels by dredging may reduce peak tidal velocity to a level below that necessary for sediment transport, causing accelerated deposition and an eventual return to an equilibrium channel depth. In contrast, a reduction of tidal prism by infilling or diking of marsh or lagoons may reduce velocities at a tidal inlet and cause deposition, leading to a smaller equilibrium cross-sectional area. Changes in channel morphology can occur on rapid time scales, with inlet cross-sectional area fluctuating by 10–15% over only a few days in response to variations in discharge due to storms or the spring-neap cycle (BYRNE *et al.*, 1975). Geologists have also noted the long-term impact on channel morphology of changes in tidal prism brought about by submergence or emergence of the tidal watershed (GARDNER and BOHN, 1980).

Qualitative effects such as these have motivated many investigators to empirically relate the cross-sectional area of tidal channels and/or inlets to flow parameters, most commonly to spring tidal prism (*e.g.*, O'BRIEN, 1969) or to peak spring discharge (*e.g.*, CHANTLER, 1974). For short inlet channels connecting bays or lagoons to the ocean, these empirical controls have been synthesized with hydrodynamic relations, resulting in stability curves for inlet cross-sectional area (ESCOFFIER, 1977; VAN DE KREEKE, 1990). In the past less attention has been paid to the morphodynamics of longer tidal channels typically associated with the interiors of tidal marshes and with the lower reaches of tidal rivers. Yet morphodynamic relations for these channelized tidal embayments are arguably simpler and more closely related to fundamental physics. Tidal channels well within embayments are isolated from the complicating effects of direct wave attack and littoral drift and are generally subjected to less severe spatial gradients in tidal amplitude and phase than are channels within tidal inlets. Recently investigators have begun to combine hydrodynamical laws with stability relations for channels within tidal basins

*94103 received 4 June 1994; accepted in revision 28 August 1994.*

(FRIEDRICHS, 1993; VAN DONGEREN and DE VRIEND, 1994). Thus it is important to recognize the distinctly different properties of stability relations for sheltered channels (*e.g.*, RIEDEL and GOURLAY, 1981) versus those more appropriate to inlets on open coasts (*e.g.*, JARRETT, 1976).

The purpose of this study is to relate channelized embayment morphology to flow properties via a physically-based mechanism, namely the "stability" shear stress ($\tau_S$) just necessary to maintain a zero gradient in net along-channel sediment transport. It is assumed that if the peak shear stress during spring tides is locally greater than $\tau_S$, then net erosion will occur, whereas if it is less than $\tau_S$ there will be net deposition. At first the problem is simplified by assuming stability is reached when grain shear stress is everywhere equal to the critical level necessary for initiation of sediment motion. Resulting theoretical relations between cross-sectional area and peak spring discharge are compared to observations from the literature taken at 242 cross-sections in 26 separate tidal systems. Next, likely causes of observed deviations from this simplest application of $\tau_S$ theory are discussed. Among tidal channels, increases in $\tau_S$ above that predicted by initiation of sediment motion are found to be correlated with increased tidal range. Along-channel variations in $\tau_S$ are hypothesized to result from systematic along-channel patterns of velocity asymmetry.

The present application of $\tau_S$ theory to tidal channel morphology involves several simplifying assumptions. Primary among them is the assertion that bottom shear stress can be related to the cross-sectionally averaged amplitude of the current. This requires density-driven currents to be at most second-order but does not require fresh water discharge to be zero or even negligible. It is also assumed that contributions to bottom stress by wind-driven currents and waves are negligible. Hence, this analysis does not address the equilibrium morphology of inlet channels exposed to significant wave activity and/or littoral drift. Another limitation of the present argument is its emphasis on non-cohesive sediment. The simplest form of $\tau_S$ theory relies in part on the Shields entrainment function for the initiation of grain motion (*e.g.*, YALIN, 1977) and other relations based exclusively on non-cohesive material. However the Shields criterion can be replaced with another critical erosion parameter based on studies of cohesive sediment (*e.g.*, DYER, 1986), and the fundamental results still remain.

## Previous Observations of Equilibrium Tidal Channels

A survey of the literature (Table 1) reveals nineteen observational studies which quantitatively relate flow along tidal channels or through tidal inlets sheltered from offshore wave activity to cross-sectional morphology (and provide sufficient data to determine both cross-sectional area and mean channel depth). Many of the authors in Table 1 noted cross-sectional area (A) to be nearly proportional to either spring tidal prism ($\Omega$) or peak discharge (Q) through relations of the form

$$A \sim \Omega^{\alpha} \text{ or } A \sim Q^{\alpha}, \tag{1}$$

where $\alpha \approx 1$, and A corresponds to the time of peak Q. If discharge is assumed to be sinusoidal, then

$$Q = \Omega\pi/T, \tag{2}$$

where T is the tidal period, and the two relations in (1) become interchangeable. However, time-series of discharge in tidal channels are often strongly asymmetric, especially in channels having large amplitude-to-depth ratios and in the upper reaches of well-mixed channels having finite fresh-water input. For the purposes of this study, direct observations of Q are preferable to estimates calculated via (2).

Figure 1 contains values for Q and A determined from information published in the sources listed in Table 1. To emphasize the distinct properties of sheltered equilibrium cross-sections relative to those exposed to ocean waves, the relationship between $\Omega$ and A found by JARRETT (1976) for U.S. Atlantic Coast inlets is superimposed (with $\Omega$ expressed in terms of Q via (2)). From Figure 1, it appears that the cross-sectional area of most sheltered tidal channel cross-sections is larger than that predicted by JARRETT, especially values of A for channels with a small Q. A similar result was found by RIEDEL and GOURLAY (1981), who compared a smaller data set of sheltered cross-sections to the empirical inlet relation of O'BRIEN (1969). The larger number of cross-sections examined here allows better constraints to be placed on the equilibrium cross-sectional area, including the roles of channel bed material, tidal range, and a physically-based concept termed the stability shear stress.

The discharges in Figure 1 are (in order of preference) either (i) taken directly from published

Table 1. *Data for 242 cross-sections of tidal channels and sheltered tidal inlets in 26 systems.*

| Location | Source | No. of Sects. | $R_{sp}$ (m) | $A \sim Q^{\alpha}$ | | $Ah^{1/6} \sim Q^{\beta}$ | |
|---|---|---|---|---|---|---|---|
| | | | | $\alpha$ | 2 s.e. | $\beta$ | 2 s.e. |
| Thames, England, UK | ALLEN (1958) | 19 | 5.2 | 1.04 | 0.04 | 1.08 | 0.05 |
| Creek off Potomac, VA, USA | LANGBEIN (1963) | 6 | 1.1 | 0.82 | 0.07 | 0.84 | 0.06 |
| Wrecked Recorder Crk., VA, USA | MYRICK and LEOPOLD (1963) | 6 | 1.0 | 1.04 | 0.15 | 1.08 | 0.15 |
| Creek off San Francisco Bay, USA | PESTRONG (1965) | 10 | 2.6 | 0.94 | 0.18 | 1.00 | 0.19 |
| Barstable*, MA, USA | REDFIELD (1965) | 6 | 3.4 | 0.91 | n.a. | 0.94 | n.a. |
| Delaware Bay, USA | HARLEMAN (1966) | 5 | 1.6 | 0.92 | 0.03 | 0.92 | 0.03 |
| Alsea, OR, USA | GOODWIN *et al.* (1970) | 7 | 2.5 | 0.65 | 0.21 | 0.66 | 0.21 |
| Siletz, OR, USA | GOODWIN *et al.* (1970) | 7 | 2.5 | 0.80 | 0.36 | 0.80 | 0.38 |
| Yaquina, OR, USA | GOODWIN *et al.* (1970) | 8 | 2.5 | 0.83 | 0.08 | 0.84 | 0.08 |
| York, VA, USA | CRONIN (1971) | 5 | 0.9 | 1.14 | 0.22 | 1.21 | 0.31 |
| Rappahannock, VA, USA | CRONIN (1971) | 16 | 0.5 | 0.98 | 0.09 | 0.99 | 0.10 |
| Potomac, VA/MD, USA | CRONIN (1971) | 17 | 0.5 | 1.06 | 0.14 | 1.12 | 0.15 |
| Ord, WA, Australia | WRIGHT *et al.* (1973) | 3 | 5.9 | 0.97 | 0.08 | 1.02 | 0.08 |
| Forth, Scotland, UK | CHANTLER (1974) | 12 | 4.9 | 0.98 | 0.11 | 1.02 | 0.12 |
| Savannah, GA, USA | CHANTLER (1974) | 7 | 2.5 | 1.34 | 0.39 | 1.41 | 0.40 |
| Sheltered inlets, Chesapeake, USA | BYRNE *et al.* (1981) | 12 | 0.4–0.5 | 0.93 | 0.27 | 1.00 | 0.27 |
| Sheltered inlets, QL, Australia | RIEDEL and GOURLAY (1981) | 3 | 2.0 | 1.12 | 0.23 | 1.22 | 0.07 |
| Western Scheldt, The Netherlands | DE JONG and GERRITSEN (1985) | 9 | 4.4 | 0.97 | 0.06 | 1.02 | 0.05 |
| Tamar, England, UK | UNCLES *et al.* (1985) | 3 | 4.7 | 1.07 | 0.11 | 1.08 | 0.11 |
| South Alligator, NT, Australia | VERTESSY (1990) | 8 | 5.8 | 1.01 | 0.05 | 1.05 | 0.06 |
| Daly, NT, Australia | VERTESSY (1990) | 9 | 6.0 | 0.91 | 0.11 | 0.89 | 0.13 |
| Adelaide, NT, Australia | VERTESSY (1990) | 8 | 3.4 | 0.73 | 0.10 | 0.71 | 0.09 |
| Sheltered inlets, Auckland, New Zealand | HUME (1991) | 5 | 2.7–3.4 | 1.01 | 0.17 | 1.09 | 0.20 |
| Usk, Wales, UK | O'CONNOR *et al.* (1991) | 29 | 12 | 0.91 | 0.10 | 0.96 | 0.11 |
| James, VA, USA | NICHOLS *et al.* (1991) | 14 | 0.9 | 0.83 | 0.09 | 0.84 | 0.09 |
| Ems, The Netherlands | DE JONGE (1992) | 8 | 2.6 | 1.04 | 0.09 | 1.08 | 0.07 |
| | | | Mean: | 0.96 | 0.05 | 1.00 | 0.06 |

*Data for individual sectons not available

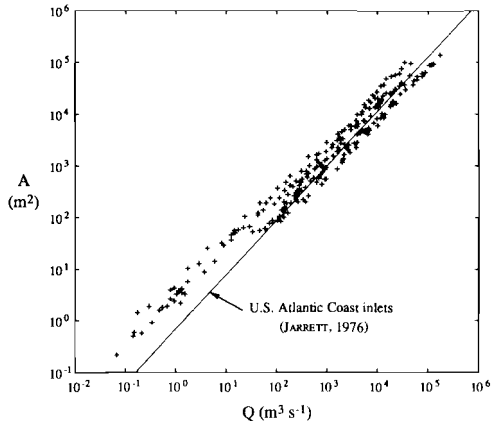


Figure 1. Observations of cross-sectional area (A) as a function of peak spring discharge (Q) at 236 sections from 25 separate sheltered tidal channels or inlet systems. Data sources are given in Table 1 (data for the six individual cross-sections of REDFIELD (1965) are not available). Superimposed is the relationship between Q and A found by JARRETT (1976) for U.S. Atlantic Coast inlets.

values of Q, (ii) calculated from published values of cross-sectionally averaged peak velocity, U, such that

$$Q = A\,U, \tag{3}$$

or (iii) calculated from published values of $\Omega$ via (2). Here Q is (ideally) defined as the magnitude of maximum discharge under spring tide conditions. Where Q corresponds to a known stage of the fortnightly cycle other than spring, then Q is scaled by the ratio of the mean spring tidal range ($R_{sp}$) to the range at the time of the discharge measurement. Where tides are of the mixed type (*i.e.*, San Francisco and Oregon in Table 1), $R_{sp}$ is defined as the difference between mean higher high water and mean lower low water. Errors in Q are estimated to be on the order of 20%.

Wherever possible, A is the area of the wetted cross-section at the time of Q. More often, however, the precise area at the time of Q is unavailable, and the cross-sectional area below mean tide level is used instead. Nonetheless, errors in the measurement of A are likely to be smaller than

errors in the measurement of Q. Here A is estimated to be accurate to within 5%. Table 1 includes only locations for which values for cross-sectionally averaged depth (h) are also available. All but two of the sources in Table 1 include h directly (or at least width, w, so that h = A/w can be calculated). Widths for the Western Scheldt sections were taken from GERRITSEN *et al.* (1991), and widths for the sheltered Australian inlets were obtained from U.S.D.M.A. charts H.O. 3451 and N.O. 74183. Finally, the seaward-most cross-section of several of the channels were purposely excluded from the analysis, either because of clear morphodynamic alteration by ocean waves and associated littoral drift (Alsen, Siletz, Yaquina, Western Scheldt, Ems) or because the seaward-most cross-section extended beyond the channelized portion of the estuary (York, Rapphannock, Potomac).

### Previous Explanations for Proportionality of A and Q

Published explanations for the near proportionality of A and Q in tidal channels include maximum entropy (LANGBEIN, 1963; MYRICK and LEOPOLD, 1963; WRIGHT *et al.*, 1973), uniform critical velocity (CHANTLER, 1974; RIEDEL and GOURLAY, 1981; BYRNE *et al.*, 1981), a form of $\tau_S$ theory based on plane bed flow (DE JONG and GERRITSEN, 1985), or merely agreement with previous empirical relationships. From an analogy to thermodynamics, the maximum entropy hypothesis states that tidal channel geometry adjusts toward a uniform distribution of energy dissipation and a minimum rate of work in the system as a whole. Uniform energy dissipation can be re-expressed as a uniform distribution of shear stress, a concept which is consistent with the present study. Minimum work, however, is not connected directly to the equations governing tidal flow and sediment motion. Thus, the maximum entropy hypothesis will not be pursued further in this paper.

In its simplest form, the critical velocity ($U_C$) hypothesis states that A adjusts until a characteristic cross-sectionally averaged $U = U_C$ causes a bottom shear stress just capable of dislodging material from the channel bed and banks (CHANTLER, 1974). If $U > U_C$, net erosion will increase the section's area, and U will decrease. Conversely, if $U < U_C$, net deposition will decrease the section's area and U will increase. This concept is more properly termed critical shear stress theory since bottom shear stress, rather than U, is dynamically linked to initiation of sediment motion. In open channel flow, boundary shear stress is strongly dependent on U and weakly dependent on depth (HENDERSON, 1966). Thus $U_C$ should vary weakly as a function of depth among tidal channels as well as along the length of individual channels. In fact, the mean value of $\alpha$ in Table 1 is a bit less than one, suggesting a slight decrease in U typically occurs as Q and depth decrease together along the length of individual channels.

KRISHNAMURTHY (1977) applied a criterion related to critical shear stress theory to his study of tidal inlet morphology in the absence of littoral drift. KRISHNAMURTHY suggested that for morphologic equilibrium, the time-averaged magnitude of bottom shear stress in the inlet should be no greater than the critical value required for sediment motion. In the study of bed load transport by tidal currents, however, it is generally agreed that the peak value of bottom shear stress is a more relevant parameter than its time-averaged magnitude (*e.g.*, BRUUN, 1967; PINGREE and GRIFFITHS, 1979).

The form of $\tau_S$ theory applied by DE JONG and GERRITSEN (1985) was originally developed for tidal inlets subject to significant littoral drift (BRUUN and GERRITSEN, 1960; BRUUN, 1967). BRUUN (1967) observed U to be 1 m/s ± 15% at seventeen sandy inlets of various sizes distributed across northern Europe and the east, west and Gulf coasts of the United States. According to BRUUN (1967), A adjusts until the total bottom shear stress produced by U flushes away the most possible sediment with the least possible frictional loss. In many inlets, $U \approx 1$ m/s is just sufficient to flatten dunes and produce a plane bed, thereby applying the maximum portion of available total shear stress directly to the bottom material. A similar mechanism may apply to tidal channels which are subjected to large inputs of sediment. However a stability theory based solely on plane bed flow is inadequate for a generalized study, for U is well below 1 m/s in many stable tidal channels.

## CRITICAL SHEAR STRESS AS A LOWER BOUND ON $\tau_S$

In this study, stability shear stress ($\tau_S$) is defined as the total bottom shear stress just necessary to maintain a zero along-channel gradient in net sediment transport. The lower bound on $\tau_S$

can be derived from the condition $\tau' = \tau'_c$, where $\tau'$ is maximum grain shear stress and $\tau'_c$ is the critical grain shear stress necessary for initiation of sediment motion. This end member is the simplest form of $\tau_s$ theory and is also known as critical shear stress theory. Critical shear stress theory has long been applied to the design of stable canals under conditions of unidirectional flow (*e.g.*, LANE, 1955; HENDERSON, 1966). Where zero scour of the canal beds and banks is desired, the limiting design condition is that $\tau'$ is no greater than $\tau'_c$ at any point of the channel boundary. However, more recent investigations of self-formed sand channels (PARKER, 1978; DIPLAS, 1990) indicate a dynamic equilibrium is possible only if $\tau'$ is slightly greater than $\tau'_c$, therefore allowing the presence of a small but finite bedload. Laboratory experiments with self-formed sand channels confirm that at equilibrium, $\tau'$ along the channel axis is up to 15% greater than $\tau'_c$ (DIPLAS, 1990).

### Application to Tidal Channels

Critical shear stress theory is used to constrain the form of equilibrium tidal channel cross-sections as a function of discharge via the following steps: (i) relating $U = Q/A$ to total bottom shear stress, $\tau$, (ii) relating $\tau$ to grain shear stress, $\tau'$, and (iii) requiring $\tau' = \tau'_c$ at equilibrium.

If flow is assumed to be steady, two-dimensional, uniform and fully rough turbulent, then the "log-layer" solution can be derived from "first-principles" via dimensional analysis (*e.g.*, YALIN, 1977):

$$u = \frac{1}{\kappa}\sqrt{\frac{\tau}{\rho}}\ln\left(\frac{z}{z_0}\right), \tag{4}$$

where $\kappa \approx 0.4$ is von Karman's constant, $\rho$ is fluid density, z is height above the bottom, and $z_0$ is a length scale related to the bottom roughness. Integrating (4) over the depth of the water column, h, gives

$$\bar{u} = \frac{1}{\kappa}\sqrt{\frac{\tau}{\rho}}\ln\left(\frac{h}{z_0 e}\right), \tag{5}$$

where $\bar{u}$ is depth-averaged velocity, and $\ln(e) = 1$. If $\tau$ is constrained to equal some critical value at equilibrium, (5) indicates that depth-averaged velocity should decrease weakly with decreased h.

An alternative equation for well-behaved flow in open channels with general properties similar to (5) is given by the more empirically based Manning-Strickler formula (*e.g.*, HENDERSON, 1966):

$$U = \frac{Q}{A} = \frac{1}{n}\sqrt{\frac{\tau}{\rho g}}\, h_R^{1/6}, \tag{6}$$

where g is the acceleration of gravity, n is Manning's friction coefficient (with metric units of $m^{1/3}s$), and $h_R$ is the hydraulic radius of the channel. Like (5), Equation (6) is directly proportional to $\tau^{1/2}$ and more weakly proportional to channel depth. Although (6) may not be as closely based on underlying physics as (5), (6) is probably better suited for application to this study. Equation (6) is based on observations of three-dimensional flow in natural rivers and large man-made channels and inherently incorporates the effects of cross-channel depth variations and channel bends. Furthermore, $\tau$ in (6) can be treated as a characteristic total bottom shear stress for the cross-section as a whole. Although the Manning-Strickler formula was developed for application to unidirectional flow, it has also been applied successfully to cross-sectionally averaged flow through tidal inlets and tidal channels (*e.g.*, MEHTA, 1978; WALLIS and KNIGHT, 1984). According to HENDERSON (1966, Table 4-2), typical values of n for natural rivers are 0.025 to 0.030 $m^{1/3}s$ for "clean and straight" channels and 0.033 to 0.040 $m^{-1/3}s$ for those that are "winding, with pools and shoals". A reasonable value of n for equilibrium tidal channels, then, would be about $0.03 \pm 0.005\ m^{-1/3}s$.

Following the suggestion of EINSTEIN (1950), total shear stress ($\tau$) is typically related to grain shear stress ($\tau'$) by $\tau = \tau' + \tau''$, where $\tau''$ is bedform drag. A survey of the literature reveals relatively few direct measurements of the ratio $\tau'/\tau$ over naturally formed bedforms in channels (Table 2). The few values that have been reported over sand range widely from less than 0.1 to about 0.7. Some of the disagreement in Table 2 results from the precise location of measurement. KAPDASLI and DYER (1986) measured $\tau'/\tau$ directly above the ripple crest, where $\tau''$ is largest. The other measurements in Table 2 are spatially averaged. In their review paper, ENGELUND and FREDSØE (1982) suggested that when $\tau'$ is only slightly greater than $\tau'_c$, $\tau'/\tau \approx 0.5$ in the presence of ripples and $\tau'/\tau \approx 0.3$ in the presence of dunes. Since spatially averaged values of $\tau'/\tau$ are needed here, a reasonable estimate for tidal channels in non-cohesive sand would be $0.4 \pm 0.2$.

For uniform, non-cohesive sediment under rough turbulent flow, dimensional analysis indicates the following relation should hold at the

Table 2. *Ratio of grain to total shear stress over naturally formed ripples and dunes.*

| Location | Source | Mean d (mm) | $\tau'/\tau$ |
|---|---|---|---|
| Laboratory flume | BAGNOLD (1963) | 0.2–0.7 | 0.2–0.5 |
| Columbia R., WA, USA | SMITH (1977) and SMITH and MCLEAN (1977) | 0.27 | 0.18–0.24 |
| Laboratory flume | ENGELUND and FREDSØE (1982) and FREDSØE (1982) | 0.2–0.9 | 0.3–0.5 |
| Laboratory flume | PAOLA (1983) | 0.2 | 0.58–0.65 |
| Tweed R., NSW, Australia | DRUERY *et al.* (1986) | 0.2–0.3 | 0.2–0.7 |
| Laboratory flume | KAPDASLI and DYER (1986) | 0.14–0.5 | 0.08–0.17* |

*Observation over ripple crest. Other observations are spatially averaged

initiation of sediment motion (e.g., YALIN, 1977):

$$\psi_C = \frac{\tau'_C}{\rho g G d}, \tag{7}$$

where G is the specific gravity of the sediment in fluid, d is the grain diameter, and the dimensionless constant $\psi_C$ is the critical Shields parameter. Experimental work by Shields (in YALIN, 1977) indicates $\psi_C = 0.05 \pm 0.01$. Combining (6) and (7) by setting $\tau' = \tau'_C$ finally gives the following upper bound on equilibrium cross-sectional geometry as a function of discharge and other externally fixed variables describing sediment and roughness characteristics:

$$A h_R^{1/6} = Qn\left(\frac{\rho g}{\tau_C}\right)^{1/2}, \tag{8}$$

where the total critical shear stress, $\tau_C$, is given by

$$\tau_C = \psi_C \rho g G d\left(\frac{\tau'}{\tau}\right)^{-1}. \tag{9}$$

## Comparison to Observations

To compare (8) to the observations in Figure 1, several additional assumptions are necessary. The density of the sediments is assumed to be well represented by quartz, for which G = 1.65. Because of the large width-to-depth ratio of the channels, it is reasonable to equate $h_R$ to the mean depth of the cross-section, h. Errors in Q are estimated to be 20%, whereas A and h are assumed accurate to within 5%. Likely variance in n and $\tau'/\tau$ are somewhat larger, as discussed in the previous section. However the least constrained variable is d.

Table 3 lists the few sources from Table 1 which provide bottom sediment information. Seven sources indicate fine-to-medium sand bottoms, three indicate significant mud, and one indicates bottom sediment which is "highly organic and black and has a texture not immediately obvious in the field" (MYRICK and LEOPOLD, 1963, p. 4). Of course (9) is not relevant to mud bottoms or for "highly organic" sediment for which the issue

Table 3. *Channel bottom sediment type at cross-sections.*

| Location | Source | Dominant Sediment Type |
|---|---|---|
| Non-cohesive | | |
| Ord | WRIGHT *et al.* (1973) | medium sand |
| Chesapeake inlets | BYRNE *et al.* (1981) | med. to fine sand |
| Queensland inlets | RIEDEL and GOURLAY (1981) | fine sand |
| Western Scheldt | DE JONG and GERRITSEN (1985) | fine sand |
| South Alligator | VERTESSY (1990) | fine sand |
| Daly | VERTESSY (1990) | med. to fine sand |
| Adelaide | VERTESSY (1990) | medium sand |
| Cohesive | | |
| Wrecked Recorder | MYRICK and LEOPOLD (1963) | "highly organic" |
| San Francisco Creek | PESTRONG (1965) | mud |
| Auckland inlets | HUME (1991) | muddy fine sand |
| James | NICHOLS *et al.* (1991) | mud |

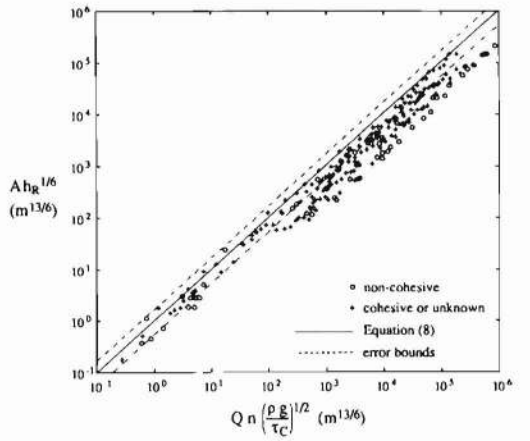


Figure 2. Observations of the cross-sectional parameter $Ah_R^{1/6}$ as a function of peak spring discharge, the total critical shear stress for non-cohesive sediments ($\tau_C$), and other externally fixed variables, superimposed on the 1:1 line given by Equation (8). Sections with bottom sediments that are known to be non-cohesive are indicated by circles.

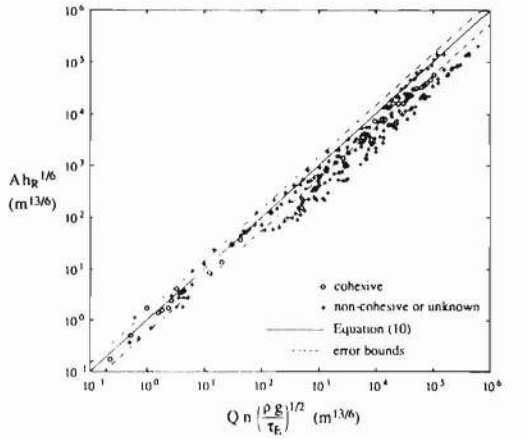


Figure 3. Observations of the cross-sectional parameter $Ah_R^{1/6}$ as a function of peak spring discharge, the critical erosion shear stress for cohesive sediments ($\tau_E$), and other externally fixed variables, superimposed on the 1:1 line given by Equation (10). Sections with bottom sediments that are known to be cohesive are indicated by circles.

of cohesion must be addressed. In applying (8)–(9) to the seven systems with bottom sediments that are known to be non-cohesive, reasonable approximations for d are used (Table 3). Otherwise, $d = 2 \pm 1$ phi is chosen, where phi $= -\log_2$(d in mm). This choice is centered at d = 0.25 mm and includes the range typically defined as fine to medium sand (1/8 to 1/2 mm). Using d = 2 phi, along with $\rho = 10^3$ kg m $^{-3}$ and the previously discussed values for $\psi_c$, G and $\tau'/\tau$, gives $\tau_C = 0.5$ N m $^{-2}$ with lower and upper error bounds of 0.1 N m $^{-2}$ and 1.1 N m $^{-2}$, respectively.

If critical shear stress theory is applied to cohesive sediment, a first-order result is given by evaluating (6) using the magnitude of critical erosion shear stress ($\tau_E$) typically observed above mud bottoms (*e.g.*, PARTHENIADES, 1965; DYER, 1986). Rather than indicating initiation of motion, $\tau_E$ represents the shear stress necessary to initiate significant erosion. The loosely held mud flocs often found at the surface of quiescent mud bottoms generally begin to move at $\tau \approx 0.05 - 0.1$ N m $^{-2}$ (DYER, 1986; KRONE, 1993), which is significantly less than typical values of $\tau_E$. In one of the most widely quoted laboratory studies of cohesive bed erosion, PARTHENIADES (1965) found rapid erosion of San Francisco Bay mud to begin at $\tau_E \approx 0.5 - 1.3$ N m $^{-2}$. LEE, *et al.* (1994) documented 152 laboratory measurements of $\tau_E$ and found published values to have a median value of 0.67 N m $^{-2}$. However the published values summarized by LEE, *et al.*, range widely, from as little as 0.01 N m $^{-2}$, to as much as 60.9 N m $^{-2}$. Though much less common than laboratory studies, in situ erosion measurements of natural cohesive beds are arguably more relavent to the present study. A recent measurement of this type was provided by SCHÜNEMANN and KÜHL (1993), who found rapid erosion of mud beds in the Elbe estuary at $\tau_E \approx 0.2$ to 1 N m $^{-2}$. Weighting our estimate slightly toward the field observations of SCHÜNEMANN and KUÜHL, $\tau_E$ is chosen here to equal 0.7 + 0.5 N m $^{-2}$.

Setting $\tau = \tau_E$ in (6) gives the following expression for cross-sectional geometry:

$$Ah_R^{1/6} = Qn\left(\frac{\rho g}{\tau_E}\right)^{1/2}. \qquad (10)$$

In evaluating (10), n is again chosen to be $0.03 \pm 0.005$ m $^{-1/3}$s, since the application of Manning's n to natural channels appears to be insensitive to bottom sediment type within the mud to sand range (HENDERSON, 1966). Equation (10) admittedly neglects the role of bedform drag; but the value of $\tau'/\tau$ applied to (8) (9) is for non-cohesive sand only and cannot confidently be used in de-

riving (10). Figures 2 and 3 display (8) and (10), along with error bounds, super-imposed on the field observations. From these figures, it is apparent that (8) and (10) produce quite similar curves.

Within error bounds, both (8) and (10) roughly predict the observed variation in $Ah_R^{1/6}$ as a function of Q and the other externally fixed variables (Figures 2 and 3); about half of the cross-sections fall within the error bars of each equation. However most of the sections fall below the lines predicted by (8) and (10), and many fall entirely below the range of likely error. As was earlier emphasized, critical shear stress theory only provides a lower bound on $\tau_S$ and, therefore, an upper bound on equilibrium cross-sectional geometry. It is reassuring to note that very few of the observations in Figures 2 and 3 fall above the error bounds.

For both cohesive and non-cohesive sediment, critical stress theory predicts that at equilibrium, tidal channel geometry will follow the relation

$$Ah_R^{1/6} \sim Q. \tag{11}$$

If regressions of the form $Ah_R^{1/6} \sim Q^\beta$ are applied to the individual systems in Table 1, then the mean value for $\beta$ is 1.00 ± 0.06 (Table 1), which is consistent with critical shear stress theory. (Plus or minus 0.06 indicates two standard errors which is approximately the 95% confidence interval.) However (11) is also consistent with any $\tau_S$ (including $\tau_S > \tau_C$) that remains nearly constant along the entire length of a given tidal channel. This can be seen by setting $\tau = \tau_S$ in (6) and then solving for $Ah_R^{1/6}$. In summary then, observations suggest that $\tau_S$ varies only slightly with distance along individual channels and that the relation $\tau_S \approx \tau_C$ (or $\tau_S \approx \tau_E$) provides reasonable upper bound for A.

## DEVIATIONS OF $\tau_S$ FROM $\tau_C$

Cross-sections from systems having small Q fall about evenly on either side of (8) and (10) in Figures 2 and 3. However cross-sections with larger Q fall consistently below the theoretical curves. This qualitative trend is confirmed statistically if a least-squares regression of the form $Ah_R^{1/6} \sim \{Q\tau_C^{-1/2}\}^\beta$ is performed on all the cross-sections in Figure 2 at once. ($\tau_C^{1/2}$ is included in the regression because $\tau_C$ can vary between systems as a function of d.) The regression gives $\beta = 0.93 \pm 0.02$, rather than $\beta = 1$ as predicted by critical shear stress theory. Yet the mean along-channel value for $\beta$ is statistically indistinguishable from one (Table 1). This supports a second form of $\tau_S$ theory, namely that $\tau_S$ tends to be uniform throughout any one channelized tidal embayment but may have a value greater than that required for initiation of sediment motion.

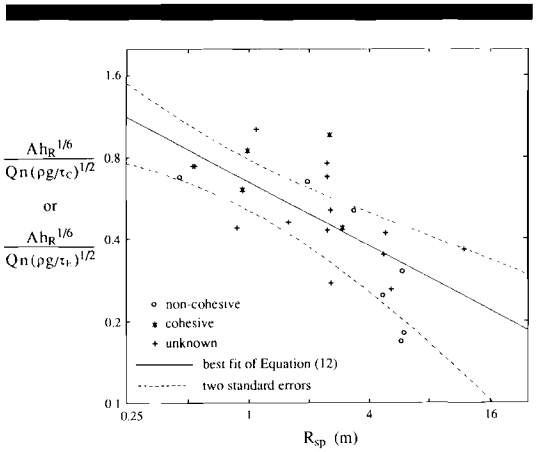


Figure 4. Observations of the cross-sectional parameter $Ah_R^{1/6}$ divided by peak spring discharge, total critical shear stress (or critical erosion stress for channels known to be cohesive) and other externally fixed variables, averaged for each tidal system, and plotted as a function of spring tidal range at the mouth of each system. Also shown is the least-squares log-log regression given by Equation (12). Sections with bottom sediments that are known to be non-cohesive or cohesive are indicated by circles or stars, respectively.

Even though large Q is associated with overprediction of $Ah_R^{1/6}$ in Figures 2 and 3, Q is probably not the variable directly responsible for the observed deviation. If the misfit were directly a result of increasing Q, then along-channel variations in Q, which can be several orders of magnitude, should also cause $\beta < 1$. Here it is postulated that among different systems, consistent deviations from a single theoretical curve are largely due to differences in spring tidal range. $R_{sp}$ varies much less than Q within individual systems and is therefore more compatible with uniform along-channel behavior of $Ah_R^{1/6}$. Thus the population-wide Q-dependent deviation may largely be the result of a fortuitous correlation between Q and $R_{sp}$.

Figure 4 displays mean (log-space) deviations from (8) as a function of $R_{sp}$ for each system in Figure 2 along with the best-fit log-log least-squares regression. The best-fit curve with standard errors is (with $R_{sp}$ in meters):

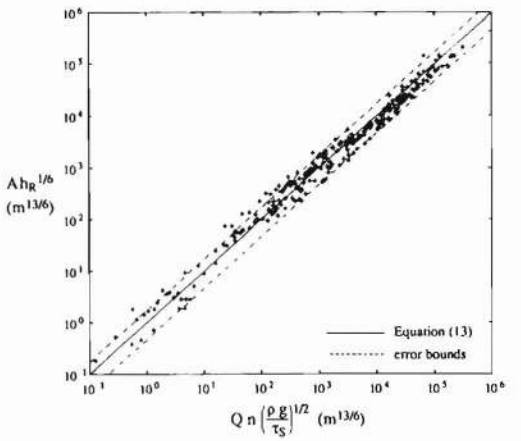


Figure 5. Observations of the cross-sectional parameter $Ah_R^{1/6}$ as a function of peak spring discharge, the stability shear stress predicted by Equation (12), and other externally fixed variables, superimposed on the 1:1 line given by Equation (13).

$$\frac{Ah_R^{1/6}}{Qn}\left(\frac{\tau_C}{\rho g}\right)^{1/2} = (0.65 \pm 0.14)R_{sp}^{\ 0.39 \pm 0.18}. \quad (12)$$

or equivalently,

$$Ah_R^{1/6} = Qn\left(\frac{\rho g}{\tau_S}\right)^{1/2}, \quad (13)$$

where

$$\tau_S = (2.3 \pm 1.0)R_{sp}^{0.79 \pm 0.35}\tau_C. \quad (14)$$

(and $\tau_E$ has been substituted for $\tau_C$ in evaluating channels with cohesive sediment). Since $\tau_C$ has already been shown to provide a reasonable lower bound on $\tau_S$, it is sensible to apply (14) only to those systems with tidal ranges large enough to give $\tau_S \geq \tau_C$. Thus (14) applies only to systems with $R_{sp} \geq \sim 0.4$ m (which includes all the channels examined in this study). Figure 5 displays (13) superimposed on all of the field observations. The observations in Figure 5 fall about evenly on either side of (13), suggesting (13) provides a reasonable mean value for cross-sectional geometry as a function of discharge, not just an upper bound.

Stability shear stress may vary with $R_{sp}$ partly due to the nature of the analysis used in this study. It is possible that the methods applied here overestimate the value of Q most relevant to equilibrium morphology in channels with large $R_{sp}$ and underestimate the most relevant Q in those with small $R_{sp}$. First, the ratio of spring to mean tidal range generally increases with tidal range. On the Potomac ($R_{sp}$ = 1 m) spring range is only 10% greater than the mean range, whereas on the Tamar ($R_{sp}$ = 4.7 m) it is 36% greater, and on the Usk ($R_{sp}$ = 12 m), it is 45% greater. If the most relevant discharge is actually a weighted average of all discharges, then use of spring discharge alone will tend to overestimate $\tau_S$ in channels with large tide ranges. Second, systems having small tide ranges may be more sensitive to morphologic change by non-tidal forces. The occasional flood or storm surge is more likely to overflow the banks of a smaller tide range channel and cause more severe erosion. Neglecting non-tidal forces may underestimate the most relevant Q (and thus underestimate $Ah_R^{1/6}$) in channels with small tide ranges.

Stability shear stress may also be a true function of spring tidal range. The larger the tidal range, the larger the likely expanse of exposed sediment in intertidal flats, which in turn may result in a greater supply of sediment to the channels. A larger supply of sediment may "clog" the channel, decrease cross-sectional area and increase U = Q/A until some $\tau_S > \tau_C$ is reached which can disperse the sediment as fast as it is supplied. Tide range is also associated with characteristic patterns of tidal distortion which should favor increased or decreased channel cross-sectional area at equilibrium. All else being equal, channels with small tide ranges tend to be ebb-dominant, whereas channels with large tide ranges tend to be flood-dominant (FRIEDRICHS and AUBREY, 1988; FRIEDRICHS and MADSEN, 1992). Ebb-dominant channels will tend to flush sediment out of a system more effectively, decreasing the level of $\tau_S$ otherwise needed to prevent shoaling. Flood-dominant systems will tend to trap sediment within a tidal channel increasing the needed level of $\tau_S$.

## ALONG-CHANNEL VARIATION IN $\tau_S$

An assumption of uniform $\tau_S$ along the length of individual tidal channels leads to the relation $Ah_R^{1/6} \sim Q$. An along-channel deviation away from uniform $\tau_S$ is indicated by a least-squares fit of $Ah_R^{1/6} \sim Q^\beta$ to data from a single system for which $\beta$ is significantly different from 1. If $\beta > 1$, $Ah_R^{1/6}$ is larger than predicted near the seaward end of the channel where Q is high and smaller than predicted near the landward end of the channel where Q is low. If the channel is stable, then $\beta > 1$ also implies that $\tau_S$ decreases in a seaward

direction. If $\beta < 1$, then the opposite is true, and $\tau_S$ decreases in a landward direction. In the previous section it was suggested that ebb- or flood-dominant discharge throughout an entire system could cause it to have a higher or lower $\tau_S$. In this section, it is suggested that spatial variations in flood- and ebb-dominance within a single system can cause analogous along-channel variations in $\tau_S$.

If the seaward portion of a tidal channel is flood-dominant while the landward portion is ebb-dominant, then a spatial convergence in the direction of maximum discharge will cause a localized increase in sediment concentration. This process has been documented previously as a "tidal turbidity maximum" in such tidal rivers as the Gironde in France (ALLEN *et al.*, 1980) and the Tamar in the U.K. (UNCLES and STEPHENS, 1989; STEPHENS *et al.*, 1992). Seaward of the turbidity maximum, flood-dominance brought about by a large tidal range-to-depth ratio (and possibly enhanced by gravitational circulation) favors landward movement of sediment; landward of the turbidity maximum, ebb-dominance brought about by fresh water discharge favors seaward movement of sediment. The resulting turbidity maximum is observed to migrate along-channel as seasonal variations in fresh water discharge cause displacement of the convergence point.

Both ALLEN *et al.* (1980) and STEPHENS *et al.* (1992) used 1-D numerical models to study the hydrodynamics associated with tidally-induced turbidity maxima. When using realistic along-channel geometries from the Gironde and the Tamar, both of their models predicted a localized increase in maximum shear stress associated with a rapid constriction in cross-sectional area. In each case, maximum shear stress was predicted to decrease landward and seaward of this point. For both the Gironde and the Tamar this fixed region of increased shear stress was found to be in the general vicinity of the previously observed, migrating turbidity maximum. Both studies suggested that this local increase in shear stress may enhance resuspension in the vicinity of the migrating turbidity maximum.

Here it is argued that the tidal turbidity maxima and locally increased stress are morphodynamically related and may help explain observed deviations from $\beta = 1$ along some stable tidal channels. Evolution towards equilibrium might proceed as follows: first, an along-channel switch from ebb- to flood-dominance favors collection of sediment at a tidal turbidity maximum; then deposition at the turbidity maximum reduces cross-sectional area, locally increasing $U = Q/A$, and; therefore, increasing maximum bottom shear stress. Ultimately, A is decreased until a locally increased $\tau_S$ is reached which prevents further deposition and effectively disperses sediment as fast as it is supplied. At equilibrium, $\tau_S$ will decrease both seaward and landward from the transition from flood- to ebb-dominance.

If a stable channel is examined seaward of the switch from ebb- to flood-dominance, then a seaward decrease in $\tau_S$ should cause $\beta > 1$ and be associated with flood-dominant discharge. Conversely, a decrease in $\tau_S$ landward of the transition should cause $\beta < 1$ and be associated with ebb-dominance. The larger the tidal range, the farther inland this transition from $\beta > 1$ to $\beta < 1$ should occur, and the more likely a fit to all the cross-sections will give $\beta > 1$. These trends seem to be borne out by Table 1 which indicates that of the eight channels macrotidal channels ($R_{sp} > 4$ m), six have $\beta > 1$. Among these eight macrotidal channels, sufficient information is available to calculate ratios of flood-to-ebb peak discharge along the Thames, Ord, Western Scheldt, Tamar, South Alligator and Daly. Average values for $Q_{flood}/Q_{ebb}$ at sections along these five tidal channels are 1.1, 2.0, 1.5, 1.2, 1.5 and 2.2, respectively, confirming an association of flood-dominance with $\beta > 1$.

If many cross-sections are available along a single macrotidal channel, it may be possible to resolve the anticipated change in morphology from $\beta > 1$ to $\beta < 1$. The two macrotidal channels in Table 1 with the largest number of cross-sections are the Usk and the Thames. Least-squares fits of $Ah_R^{1/6} \sim Q^\beta$ to the seaward portions of these two channels indeed give $\beta > 1$, whereas fits to the landward portion give $\beta < 1$ (Figure 6). Thus the relatively low value of $\beta = 0.96$ for the entire Usk may be due to a sampling of cross-sections on both sides of the transition from flood- to ebb-dominance. ALLEN (1958) and O'CONNER *et al.* (1991) also noted an along-channel discontinuity in the relationship between Q and A along the Thames and Usk, respectively, which they qualitatively associated with the influence of riverine versus tidal processes. In this paper a more physically-based mechanism is suggested, namely morphodynamic feedback between temporal and spatial asymmetries in bed stress in the vicinity of the tidal turbidity maximum.

All of the tidal channels subject to tides of mixed

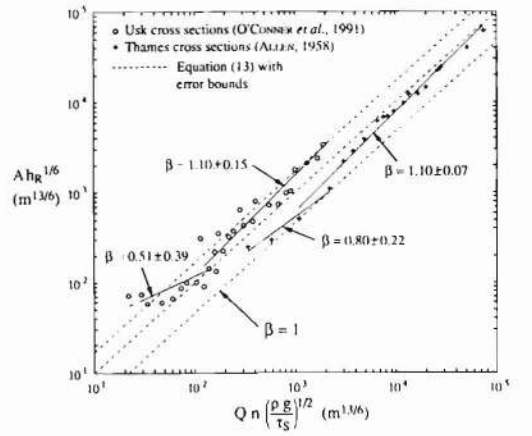


Figure 6. Observations along the Usk and Thames of the cross-sectional parameter $Ah_R^{1/6}$ as a function of peak spring discharge, the stability shear stress predicted by Equation (12), and other externally fixed variables, superimposed on the 1:1 line given by Equation (13). Also shown are least-squares log-log regressions for $\beta$ along the landward and seaward portions of the estuary.

type (San Francisco and the three Oregon channels), have $\beta \leq 1$ (Table 1). This may be due to a systematic association of mixed tides with ebb-dominance. In a mixed-tide regime, the lower low tide usually follows the higher high tide, causing the largest changes in tidal elevation to occur consistently during the ebb. However this consideration is merely speculative. The unusually low values for $\beta$ in the Oregon channels could also result from choking of the seaward end by littoral drift even beyond the most seaward cross-section (the seaward-most section of each Oregon channel has already been dropped from the analysis).

## SUMMARY AND CONCLUSIONS

A survey of the literature allows estimates of peak spring discharge and cross-sectional geometry at 242 sections in 26 separate tidal systems. Previous explanations for the near proportionality of cross-sectional area (A) and discharge (Q) include maximum entropy, uniform critical velocity, and a propensity toward plane bed flow. The purpose of this study is to relate the morphology of sheltered tidal channels to flow properties via a more robust, physically-based mechanism, namely the stability shear stress ($\tau_S$) just necessary to maintain a zero gradient in net along-channel sediment transport. It is assumed that if $\tau > \tau_S$, net erosion will occur, increasing A, and reducing $\tau \sim (Q/A)^2$ back toward $\tau_S$. If $\tau < \tau_S$ there will be net deposition, reducing A and increasing $\tau$ toward $\tau_S$.

A theoretical lower bound on $\tau_S$ (and an upper bound on A) for channels floored by non-cohesive sediment is provided by the condition $\tau' = \tau'_C$, where $\tau'$ is maximum grain shear stress and $\tau'_C$ is the critical grain shear stress necessary for initiation of sediment motion. Critical shear stress theory is applied to equilibrium tidal channel geometry by (a) relating $U = Q/A$ to $\tau$ via the Manning-Strickler equation, (b) relating total shear stress, $\tau$, to $\tau'$ via empirical ratios from the literature, and (c) determining $\tau' = \tau'_C$ from the Shields criterion for the initiation of sediment motion. For cohesive sediments, $\tau$ is assumed to equal $\tau_E$ at equilibrium, where $\tau_E$ is the magnitude of critical erosion shear stress typically observed above mud bottoms.

Comparison to observations indicates $\tau' = \tau'_C$ and $\tau = \tau_E$ do a reasonable job of predicting equilibrium cross-sectional geometry in general and an excellent job of predicting the upper bound on likely geometry. In either case, uniform critical values for $\tau$ predict that at equilibrium, along-channel geometry will follow the relation $Ah_R^{1/6} \sim Q$, where $h_R$ is the hydraulic radius. Along-channel regressions of the form $Ah_R^{1/6} \sim Q^\beta$ give a mean observed value for $\beta$ of $1.00 + 0.06$, which is consistent with critical shear stress theory.

Although along-channel geometry agrees, on average, with the prediction $Ah_R^{1/6} \sim Q$, the uniform $\tau_S$ appropriate to individual systems can vary widely above that predicted by $\tau' = \tau'_C$ or $\tau = \tau_E$. Observed $\tau_S$ is found to vary among systems according to the relation $\tau_S \approx 2.3\, R_{sp}^{0.79} \tau_C$, where $R_{sp}$ (in meters) is the spring tidal range, and $\tau_C$ is the total shear stress when $\tau' = \tau'_C$. $\tau_S$ may vary with $R_{sp}$ because of an increase in exposed flats associated with large $R_{sp}$. An increased sediment supply may "clog" the channel, increasing the $\tau_S$ necessary for effective sediment dispersal. Also, small $R_{sp}$ favors ebb-dominance, whereas large $R_{sp}$ favors flood-dominance. Ebb-dominance may aid the flushing of sediment, decreasing $\tau_S$, whereas flood-dominance may enhance shoaling and increase $\tau_S$.

Observed deviations from $Ah_R^{1/6} \sim Q$ along individual channels are associated with a convergence in discharge asymmetry. It is hypothesized that a spatial convergence in the direction of max-

imum discharge may cause net deposition, a reduction in A, and a local increase in U = Q/A until some larger $\tau_S$ is reached which prevents further deposition. In a stable channel, $\tau_S$ will then decrease both seaward and landward of the convergence point. If a regression of the form $Ah_R^{1/6} \sim Q^\beta$ is applied along such a channel, one should find $\beta > 1$ associated with flood-dominance seaward of the maximum in $\tau_S$ and $\beta < 1$ associated with ebb-dominance landward. Geometries and discharge asymmetries along several channels are observed to be consistent with this pattern.

## ACKNOWLEDGMENTS

D. Aubrey, N. Kobayashi, D. Lynch, O. Madsen, and A. Mehta provided helpful comments on the manuscript. This work was supported by the National Science Foundation, under grant OCE 91-02429. VIMS contribution number 1887.

## LITERATURE CITED

ALLEN, F.H., 1958. Discussion on Flow in alluvial channels with sandy mobile beds, by G. Lacey. *Proceedings of the Institution of Civil Engineers*, 11, 223–225.

ALLEN, G.P.; SALOMON, J.C.; BASSOULLET, P.; DU PENHOAT, Y., and DE GRANDPRÉ, C. 1980. Effects of tides on mixing and suspended sediment transport in macrotidal estuaries. *Sedimentary Geology*, 26, 69–90.

BAGNOLD, R.A., 1963. Beach and nearshore processes, part I: mechanics of marine sedimentation. *In*: HILL, M.N., (ed.), *The Sea*. New York: Wiley, pp. 507–528.

BRUUN, P., 1967. Tidal inlet housekeeping. *Journal of the Hydraulics Division, A.S.C.E.*, 93, 167–184.

BRUUN, P., 1978. *Stability of Tidal Inlets, Theory and Engineering*. New York: Elsevier, 506 p.

BRUUN, P., and GERRITSEN, F., 1960. *Stability of Tidal Inlets*. Amsterdam: North Holland Publishing, 130 p.

BYRNE, R.J.; BULLOCK, P., and TYLER, D.G., 1975. Response characteristics of a tidal inlet: a case study. *In*: CRONIN, L.E., (ed.), *Estuarine Research, Volume II: Geology and Engineering*. New York: Academic Press, pp. 201–216.

BYRNE, R.J.; GAMMISCH, R.A., and THOMAS, G.R., 1981. Tidal prism-inlet area relations for small tidal inlets. In: *Proceedings of the 17th International Conference on Coastal Engineering*. New York: American Society of Civil Engineers, pp. 2517–2533.

CHANTLER, A.G., 1974. The applicability of regime theory to tidal watercourses. *Journal of Hydraulic Research*, 12, 181–191.

CRONIN, W.B., 1971. Volumetric, areal, and tidal statistics of the Chesapeake Bay estuary and its tributaries. *Chesapeake Bay Institute, Special Report 20*, Johns Hopkins University, 135 p.

DE JONG, H., and GERRITSEN, F., 1985. Stability parameters of the Western Scheldt estuary. In: *Proceedings of the 19th International Conference on Coastal Engineering*. New York: American Society of Civil Engineers, pp. 3079–3093.

DE JONGE, V.N., 1992. Tidal flow and residual flow in the Ems estuary. *Estuarine, Coastal and Shelf Science*, 34, 1–22.

DIPLAS, P., 1990. Characteristics of self-formed straight channels. *Journal of Hydraulic Engineering, A.S.C.E.*, 116, 707–728.

DRUERY, B.M.; BRITTON, G.W., and GREENTREE, G.S., 1984. Discussion on Shape and dimensions of stationary dunes in rivers, by J. Fredsøe. *Journal of the Hydraulics Division, A.S.C.E.*, 110, 855–857.

DYER, K.R., 1986. *Coastal and Estuarine Sediment Dynamics*. New York: Wiley, 342 p.

EINSTEIN, H.A., 1950. The bed-load function for sediment transportation in open channel flows. *U.S. Department of Agriculture, Technical Bulletin No. 1026*, Washington, D.C.

ENGELUND, F., and FREDSØE, J., 1982. Sediment ripples and dunes. *Annual Review of Fluid Mechanics*, 14, 13–37.

ESCOFFIER, F.F., 1977. Hydraulics and stability of tidal inlets. *U.S. Army Coastal Engineering Research Center, G.I.T.I. Report 13*, Vicksburg, Mississippi, 72 p.

FREDSØE, J., 1982. Shape and dimensions of stationary dunes in rivers. *Journal of the Hydraulics Division, A.S.C.E.*, 108, 932–947.

FRIEDRICHS, C.T., 1993. Morphodynamics and Hydrodynamics of Shallow Tidal Channels and Intertidal Flats. Unpublished Ph.D. dissertation, Massachusetts Institute of Technology-Woods Hole Oceanographic Institution Joint Program, Woods Hole, 218 p.

FRIEDRICHS, C.T., and AUBREY, D.G., 1988. Non-linear tidal distortion in shallow well-mixed estuaries: a synthesis. *Estuarine, Coastal and Shelf Science*, 27, 521–545.

FRIEDRICHS, C.T., and MADSEN, O.S., 1992. Nonlinear diffusion of the tidal signal in frictionally dominated embayments. *Journal of Geophysical Research*, 97, 5637–5650.

GARDNER, L.R. and BOHN, M., 1980. Geomorphic and hydraulic evolution of tidal creeks on a subsiding beach ridge plain, North Inlet, S.C. *Marine Geology*, 34, M91–M97.

GERRITSEN, F.; DE JONG, H., and LANGERAK, A., 1991. Cross-sectional stability of estuary channels in the Netherlands. *In*: EDGE, B.L., (ed.), *Proceedings of the 22nd International Conference on Coastal Engineering*. New York: American Society of Civil Engineers, pp. 2922–2935.

GOODWIN, C.R; EMMETT, E.W., and GLENNE, B., 1970. Tidal study of three Oregon estuaries. *Oregon State University Engineering Experiment Station, Bulletin No. 45*, Corvallis, Oregon, 45 p.

HARLEMAN, D.R.F., 1966. Tidal dynamics in estuaries, part II: real estuaries. *In*: IPPEN, A.T., (ed.), *Estuary and Coastline Hydrodynamics*. New York: McGraw-Hill, pp. 522–545.

HENDERSON, F.M., 1966. *Open Channel Flow*. New York: Macmillan, 522 p.

HUME, T.M., 1991. Empirical stability relationships for estuarine waterways and equations for stable channel design. *Journal of Coastal Research*, 7, 1097–1111.

JARRETT, J.T., 1976. Tidal prism—inlet area relationships. *U.S. Army Coastal Engineering Research Center, G.I.T.I. Report 3*, Vicksburg, Mississippi, 32 p.

KAPDASLI, M.S., and DYER, K.R., 1986. Threshold conditions for sand movement on a rippled bed. *Geo-Marine Letters*, 6, 161–164.

KRISHNAMURTHY, M., 1977. Tidal prism of equilibrium inlets. *Journal of the Waterway, Port, Coastal and Ocean Division, A.S.C.E*, 103, 423–432.

KRONE, R.B., 1993. Sedimentation revisited. *In*: MEHTA, A.J., (ed.), *Nearshore and Estuarine Cohesive Sediment Transport, Coastal and Estuarine Studies Vol. 42.* Washington, D.C.: American Geophysical Union, pp. 108–125.

LANGBEIN, W.B., 1963. The hydraulic geometry of a shallow estuary. *Bulletin of the International Association of Scientific Hydrology*, 8, 84–94.

LANE, E.W., 1955. Design of stable channels. *Transactions, American Society of Civil Engineers*, 120, 1234–1260.

LEE, S.-C.; MEHTA, A.J., and PARCHURE, T.M., 1994. Cohesive sediment erosion: parts I and II. *Coastal and Oceanographic Engineering Department, Report UFL/COEL/MP-94/02*, University of Florida, Gainesville, 68 p.

MEHTA, A.J., 1978. Bed friction characteristics of three tidal entrances. *Coastal Engineering*, 2, 69–83.

MYRICK, R.M. and LEOPOLD, L.B., 1963. Hydraulic geometry of a small tidal estuary. *U.S. Geological Survey Professional Paper*, 442-B, 18 p.

NICHOLS, M.M.; JOHNSON, G.H., and PEEBLES, P.C., 1991. Modern sediments and facies model for a microtidal coastal plain estuary, the James Estuary, Virginia. *Journal of Sedimentary Petrology*, 61, 883–899.

O'BRIEN, M.P., 1969. Equilibrium flow areas of inlets on sandy coasts. *Journal of the Waterways and Harbors Division, A.S.C.E.*, 95: 43–52.

O'CONNOR, B.; NICHOLSON, J., and RAYNER, R., 1991. Estuary geometry as a function of tidal range. *In*: EDGE, B.L., (ed.), *Proceedings of the 22nd International Conference on Coastal Engineering.* New York: American Society of Civil Engineers, pp. 3050–3062.

PAOLA, C., 1983. Flow and Skin Friction Over Natural Rough Beds. Unpublished Ph.D. dissertation, Massachusetts Institute of Technology-Woods Hole Oceanographic Institution Joint Program, Woods Hole, 347 p.

PARKER, G., 1978. Self-formed straight rivers with equilibrium banks and mobile bed, part 1: the sand-silt river. *Journal of Fluid Mechanics*, 89, 109–125.

PARTHENIADES, E., 1965. Erosion and deposition of cohesive soils. *Journal of the Hydraulics Division, A.S.C.E.*, 91, 105–139.

PESTRONG, R., 1965. The development of drainage patterns on tidal marshes. *Stanford University Publications in the Geological Sciences*, Vol. 10, No. 2, Stanford, California, 87 p.

PINGREE, R.D. and GRIFFITHS, D.K., 1979. Sand transport paths around the British Isles resulting from $M_2$ and $M_4$ tidal interactions. *Journal of the Marine Biological Association of the U.K.*, 59, 497–513.

REDFIELD, A.C., 1965. Ontogeny of a salt marsh. *Science*, 147, 50–55.

RIEDEL, H.P. and GOURLAY, M.R., 1981. Inlets/estuaries discharging into sheltered waters. In: *Proceedings of the 17th International Conference on Coastal Engineering.* New York: American Society of Civil Engineers, pp. 2550–2564.

SCHÜNEMANN, M. and KÜHL, H., 1993. Experimental investigations of the erosional behavior of naturally formed mud from the Elbe estuary and adjacent Wadden Sea, Germany. *In*: MEHTA, A.J., (ed.), *Nearshore and Estuarine Cohesive Sediment Transport, Coastal and Estuarine Studies Vol. 42.* Washington, D.C.: American Geophysical Union, pp. 314–330.

SMITH, J.D., 1977. Modeling of sediment transport on continental shelves. *In*: GOLDBERG, E.D., (ed.), *The Sea, Vol. 6.* New York: Wiley, pp. 539–577.

SMITH, J.D. and MCLEAN, S.R., 1977. Spatially averaged flow over a wavy surface. *Journal of Geophysical Research*, 82: 1735–1746.

STEPHENS, J.A.; UNCLES, R.J.; BARTON, M.L., and FITZPATRICK, F., 1992. Bulk properties of intertidal sediments in a muddy, macrotidal estuary. *Marine Geology*, 103, 445–460.

UNCLES, R.J.; ELLIOTT, R.C.A., and WESTON, S.A., 1985. Lateral distributions of water, salt and sediment transport in a partly mixed estuary. *In*: EDGE, B.L., (ed.), *Proceedings of the 19th International Conference on Coastal Engineering.* New York: American Society of Civil Engineers, pp. 3067–3077.

UNCLES, R.J. and STEPHENS, J.A., 1989. Distributions of suspended sediment at high water in a macrotidal estuary. *Journal of Geophysical Research*, 94, 14,395–14,405.

VAN DE KREEKE, J., 1990. Can multiple tidal inlets be stable? *Estuarine, Coastal and Shelf Science*, 30, 261–273.

VAN DONGEREN, A.R. and DE VRIEND, H.J., 1994. A model of morphological behaviour of tidal basins. *Coastal Engineering*, 22, 287–310.

VERTESSY, R.A., 1990. Morphodynamics of Macrotidal Rivers in Far Northern Australia. Unpublished Ph.D. dissertation, Australian National University, Canberra, 372 p.

WALLIS, S.G., and KNIGHT, D.W., 1984. Calibration studies concerning a one-dimensional numerical tidal model with particular reference to resistance coefficients. *Estuarine, Coastal and Shelf Science*, 19, 541–562.

WRIGHT, L.D.; COLEMAN, J.M., and THOM, B.G., 1973. Processes of channel development in a high-tide range environment: Cambridge Gulf-Ord River delta, Western Australia. *Journal of Geology*, 81, 15–41.

YALIN, M.S., 1977. *Mechanics of Sediment Transport* (2nd edition). New York: Pergamon, 298 p.